Detection of the Misalignment Fault in Non-Electric Rotating Machines Through the Current Signal of a Brushless Direct Current Motor

Ali Bolourian [1], Abbas Ehsani-Seresht[2*], Reza Roshanfekr [3]

Abstract—**One of the most common causes of vibration in rotating machines is the misalignment fault. The Motor Current Signature Analysis (MCSA) is an excellent method for the detection of the misalignment fault on those electric machines whose current signals are practically available. This paper aims to extend the application of the MCSA method to non-electric rotating systems for the detection of the misalignment fault between the driver machine and the driven machine. For this, a small brushless direct current (BLDC) motor was connected to the driver machine. Then, by using the Fast Fourier Transform and Wavelet Packet Transform the current signal of the BLDC motor was analyzed to detect the misalignment fault. In addition, a fault detection indicator was provided using the energy of the current signal. For the evaluation of the proposed method, an experimental setup was provided. The driver machine of the setup was an induction machine. So, it was possible to investigate the misalignment fault through both the BLDC motor and the induction motor. The results showed that the misalignment fault can be detected by the current signal of the BLDC motor as well as the current signal of the driver machine.**

Index Terms— **Condition monitoring, Fault detection, Fast Fourier Transform, Wavelet packet transform.**

I. INTRODUCTION

Rotating machines have been found in widespread use in power plants, steel plants, and petrochemicals. Thus, the performance of these large industries depends upon the correct and continuous operation of these rotating machines. Sudden and unplanned interruptions of these rotating machines will result in substantial financial losses. Therefore, it is essential to use condition-monitoring strategies for these systems to detect their faults in the early stages. Rotating systems are exposed to a variety of mechanical faults, including bearing faults, eccentricity, shaft bending, shaft cracking, unbalance, and misalignment. Among these faults, the misalignment fault is important, so more than 70% of vibrations of rotating systems are due to misalignment [1].

Misalignment occurs when there are more than two bearings in one shaft, such as when the two machines are connected via a coupling. Misalignment may be parallel, angular, or combined [2]. Different kinds of couplings including flexible and universal couplings are used to prevent the deleterious effects of misalignment on the bearings.

Vibration analysis is a famous method used to detect misalignment in rotating systems. In 1976 gibbons analysed the forces and torques of misaligned flexible couplings [3]. In a single run-down, Sinha et al. suggested a method to use the vibration signal to identify the unbalance and misalignment forces [4]. Through his research on cylinder and three-lobe journal bearings, Prabhu demonstrated that the second harmonic of the sound signal changes as the angular misalignment increases [5]. In their analytical model of a straightforward rotating system, Bahaloo et al. showed that the second harmonic of the system is the key characteristic that underlies both parallel and angular misalignments [6]. The angular misalignment of shafts in the gearbox was investigated by Chacon et al. using the acoustic emission method [7]. Additionally, there are numerous other studies that have employed acoustic emission for the identification of misalignment faults [8–10]. Sarkar et al. used finite element analysis for different types of misalignment on multi-disk rotors supported by oil-film bearings [11]. Xu and Marangoni developed a model for a motor-flexible coupling-rotor system and concluded that the angular misalignment causes the system to vibrate at even multiple frequencies of the motor speed [12]. Hili et al. proposed a finite element model for angular and parallel misalignments and concluded that for angular misalignment the first and second harmonics of the running frequency are dominant. In addition, they found that for parallel misalignment multiple harmonics of the running frequency are excited [13].

Besides the vibration analysis for the detection of misalignment in rotating machines, motor current signature analysis (MCSA) has also been developed in recent years by researchers due to its accessibility, low-price sensors, and its robustness to environmental conditions [14]. MCSA has been used by several research groups for the detection of mechanical faults and they have got acceptable results [15-19]. Daviu and Popaleny used a transient current signature analysis to diagnose mechanical faults such as misalignment [20].

Detection of misalignment by the MCSA method is only possible in rotating systems driven by electrical machines.

1- A. Bolourian is with the Department of Mechanical Engineering, Hakim Sabzevari University, Sabzevar, Iran
2- A. Ehsani-Seresht is with the Department of Mechanical Engineering, Hakim Sabzevari University, Sabzevar, Iran
3- R. Roshanfekr is with the Department of Electrical Engineering, Hakim Sabzevari University, Sabzevar, Iran
Corresponding author: a.ehsaniseresht@hsu.ac.ir

However, there are many rotating systems in large industries that do not work with electric power. Thus, the MCSA method for such systems is not applicable.

In this paper, the application of MCSA on non-electric rotating systems using an externally mounted electric motor was investigated. A suitable candidate for the external electric motor is a BLDC motor due to its small size and its robustness. In this method, the BLDC motor was connected to the driver machine to rotate with the speed of the driver machine. Therefore, the BLDC motor acts as an electric generator and produces an electric current. Current sensors are used to measure this electric current. Because the BLDC motor senses the speed fluctuations of the driver machine, the output current of the BLDC motor demonstrates the probable faults of the system. To prevent from false harmonics in the current signal of the BLDC motor, the connection of the BLDC motor to the driver machine is carefully aligned.

To evaluate the results obtained from the BLDC motor, in this study, an experimental setup was used. The driver machine of the setup is a three-phase induction motor. Therefore, for misalignment conditions, the results of the MCSA for both motors are compared together.

II. THEORETICAL BACKGROUND

A. Effect Of Misalignment on A Rotating System

Based on experimental and theoretical investigations [21, 22], the misalignment fault between two rotating machines causes vibration at the low harmonics of the rotational frequency of the system as follows:

$$f_{Mv} = k f_r \qquad (1)$$

Where f_r is the rotational frequency of the system and k is a positive integer.

If the driver machine of the system is an electric motor, then the misalignment fault affects the current signal of the driver machine. The characteristic frequencies of the misalignment faults occur through the sidebands of the main frequency of the system as follows [14, 23, 24]:

$$f_{Mc} = f_s \pm k f_r \qquad (2)$$

Were, send main frequency of the electric machine.

B. Detection Of Faults Through BLDC

Fig. 1 shows a schematic representation of the MCSA method for rotating systems with an electric machine as a driver. In this method, the current signals from an induction motor are measured and analysed to detect different faults in the system.

It is feasible to attach an electric engine to a rotating system's non-electric driver machine in order to monitor the system's speed fluctuations. The technique for measuring the current signal from a BLDC motor is schematically shown in Fig. 2. In this diagram, the non-electric driver machine serves as the system's primary engine, while the BLDC motor serves as a generator. The outputs of the BLDC motor are equipped with three current gauges.
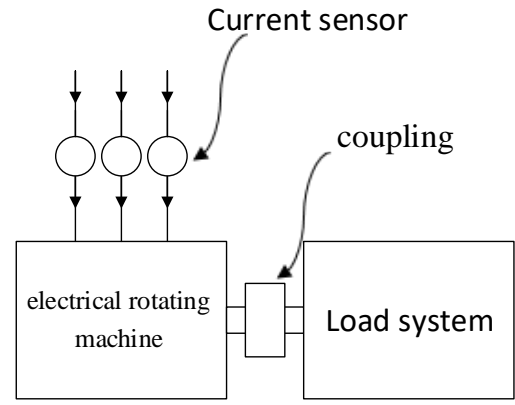
Fig. 1. Schematic representation of an electrical rotating machine for acquiring electric driver current signals
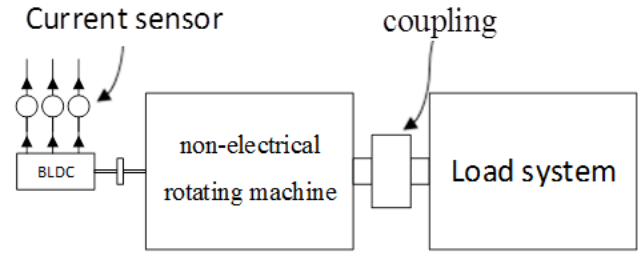
Fig. 2. Schematic representation of a non-electrical rotating machine for acquiring BLDC current signals

C. Fast Fourier Transforms

Most of the faults in rotating machines cause specific frequency signatures in vibration and current signals. These faults can be detected by the signals in the frequency domain. The Fourier Transform (FT) is a famous method to analyze the signals in the frequency domain. The FT decomposes each signal into a series of complex exponential functions with different frequencies. The Fourier transform function was defined as [24]:

$$X(\omega) = \int_{-\infty}^{+\infty} x(t) * e^{-i\omega t} dt \qquad (3)$$

Where, t represents the time, f is frequency, x is the signal in the time domain, and X is the signal in the frequency domain. The FT was used for time-continuous signals. However, the signals measured by the condition monitoring systems are discrete signals discrete-time time signals, and the discrete Fourier transform (DFT) was used to transform the signal to the frequency domain. DFT can be expressed as:

$$X_k = \sum_{n=0}^{N-1} x_n e^{-i2\pi kn/N} \quad k = 0: N - 1 \qquad (4)$$

Despite the advantages of the DFT in processing signals, it is computationally inefficient. The Fast Fourier transform (FFT) overcomes this limitation and computes the DFT in a fast method.

D. Wavelet Packet Transform

The wavelet transform (WT) is another method that provides the capability of analysis of the signals in the frequency domain. The WT decomposes a time domain signal into approximate

and detailed signals. The approximate signal includes the low-frequency contents of the main signal and the detail signal

contains the high-frequency features of the main signal. By the WT, the low-frequency signal itself has decomposed into approximate and detailed signals again. This signal decomposition can take several steps. The WT steps were illustrated in Fig. 3. Due to the signal decomposition method proposed in the WT method, low-frequency faults are detected more precisely than high-frequency faults. However, most of the faults in rotating machines occur in high-frequencies, and the WT is weak at high-frequency separation. The Wavelet packet transform analysis complements the WT.
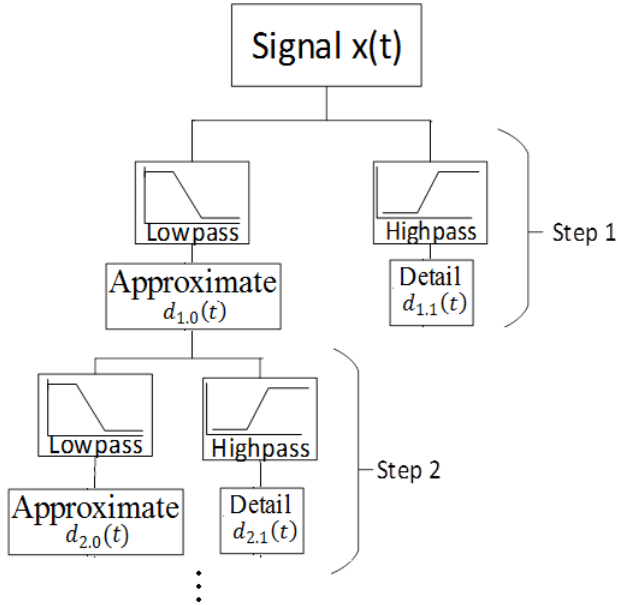
Fig. 3.   Block diagram of DWT

As a modern tool for signal processing, the Wavelet Packet Transform (WPT) has received a great deal of attention in condition monitoring applications [25-29]. In comparison to WT, The WPT not only decomposes the approximate signal into two other signals but also divides the detail signal into two new signals. Fig. 5 demonstrates the WPT for a time domain signal. The WPT enables a more accurate analysis of faults with high-frequency characteristics. To perform a WPT on a time signal at a given level j, the functions were defined as follows [29]:

$$d_{j+1.2n} = \sum_m h(m - 2k)d_{j.n} \qquad (5)$$

$$d_{j+1.2n+1} = \sum_m g(m - 2k)d_{j.n} \qquad (6)$$

Where, g and h are high and low pass filters, respectively, known as Quadrature Mirror Filters (QMF). Also, $d_{j.n}$ denotes the wavelet coefficients at the j level, n^{th} sub-band, respectively, and m is the number of the wavelet coefficient. According to Fig. 4, if a given signal was decomposed into two levels, four sub-bands are produced, covering every four bands of frequency information [29]. Then the most suitable frequency band that has the fault frequency characteristic was selected and by feature extraction, an indicator is obtained to diagnose the fault.
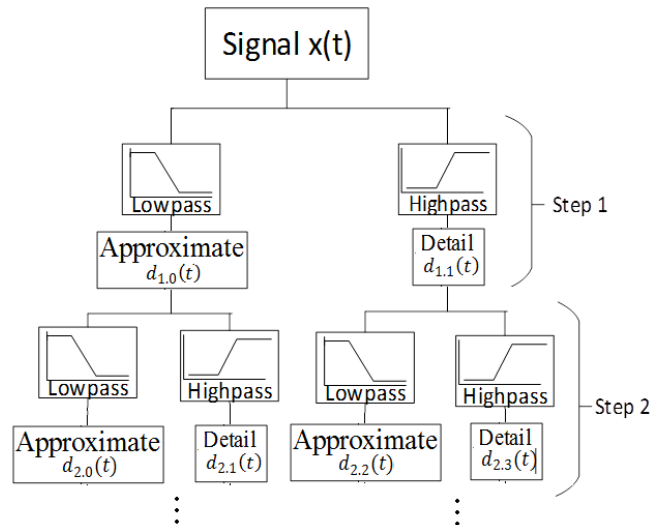
Fig. 4.   Illustration of wavelet packet transforms.

III. EXPERIMENTAL SETUP

The experimental setup, as shown in Fig. 5, includes a two-pole, three-phase squirrel cage induction motor (IM) as a driver machine that connects to the load system via a jaw coupling. The loading system is a three-phase synchronous generator. In addition, a 14-pole small-scale BLDC motor was coupled to the driver to detect the misalignment fault between the driver machine and the load system. Although the system could operate with a non-electric driver machine, the IM offers the chance to evaluate the outcomes of the IM and the BLDC motor. The three stages of the IM and the BLDC motor's current signals were measured using six current sensors. The DAQ card sends the current signals to the computer, where MATLAB software is used to analyze the signals.

The experiments are performed in three different conditions including healthy condition, minor parallel misalignment (level 1), and major parallel misalignment (level 2). For each condition, the experiments were performed in no-load, half-load, and full-load conditions. To provide minor parallel misalignment, a 1 mm metal sheet was placed under the IM. Also, for major parallel misalignment, a 2 mm metal sheet was placed under the IM. For all experiments, the current signals of the IM and the BLDC motor were measured with a sampling rate of 5 kHz.
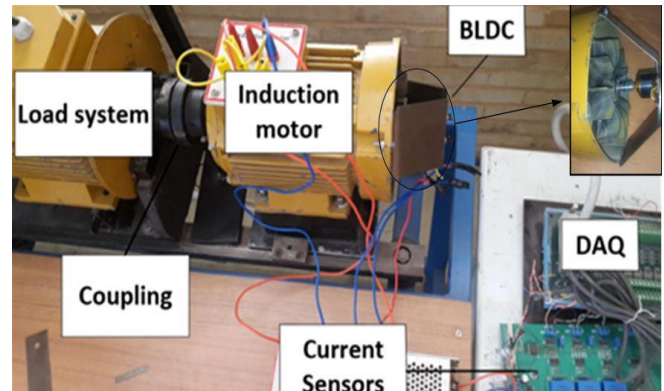
Fig. 5. Experimental set-up

IV. RESULTS

A. Fast Fourier Transform

In Fig. 6, a representative current signal of the BLDC motor and the IM is shown. The main frequency of the BLDC motor is higher than the IM because the BLDC motor has 14 poles while the IM has 2 poles. For this experiment, the angular velocity of the system for the no-load condition was $v = 2998\ rpm$. Therefore, the main frequencies of the IM and the BLDC motor are 49.97 Hz and 349.77 Hz, respectively. In addition, for the misalignment fault, the characteristic frequencies of the current signal for the IM and the BLDC motor are obtained from (2). Some of these frequencies are listed in Table I and Table II.
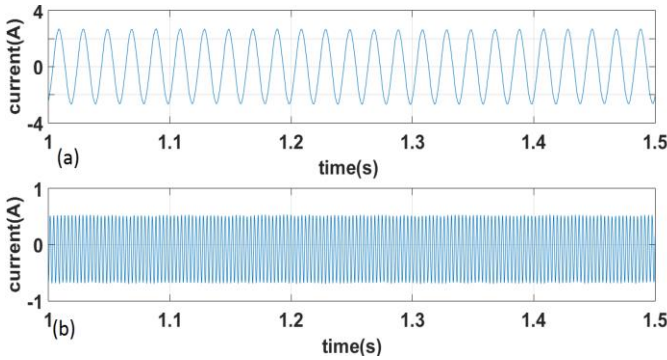
Fig. 6. (top) IM current signal (bottom) BLDC motor current signal

TABLE I

Characteristic Frequencies of the IM's Current Signal for Parallel Misalignment

k	f_{rf}
1	99.7
2	149.4
3	199.1
4	248.8

TABLE II

Characteristic Frequencies of the BLDC Motor's Current Signal for Parallel Misalignment

k	f_{rf}	k	f_{rf}
-1	298.45	1	397.94
-2	248.71	2	447.68
-3	198.97	3	497.42
-4	149.22	4	547.17

Fig.7 shows the current signal of the IM in the frequency domain for health conditions. In addition, Fig. 8 and 9 show the frequency content of the IM's current signal in level-1 and level-2 faults. Comparing Fig. 8 and 9 with Fig. 7 demonstrates that in fault conditions the current signal has frequency contents that are determined in Table I. The amplitude of each harmonic is given in Fig. 10 for healthy, level-1, and level-2 conditions. Among them, the first harmonic related to K=1 has better results to detect the fault.
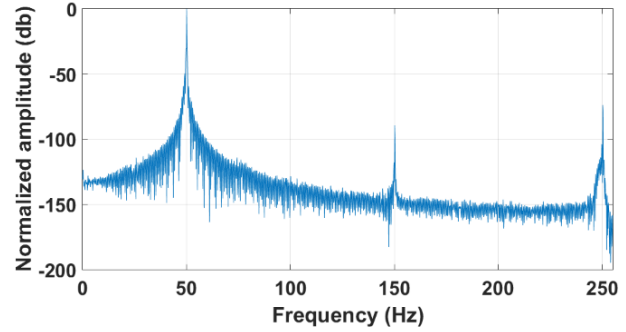
Fig. 7. Normalized spectrum of the IM's current for the healthy condition
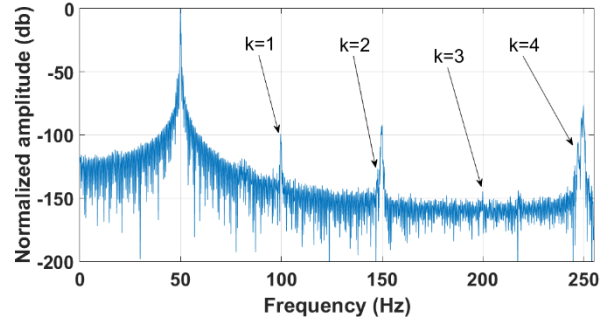
Fig. 8. Normalized spectrum of the IM's current for level-1 misalignment condition
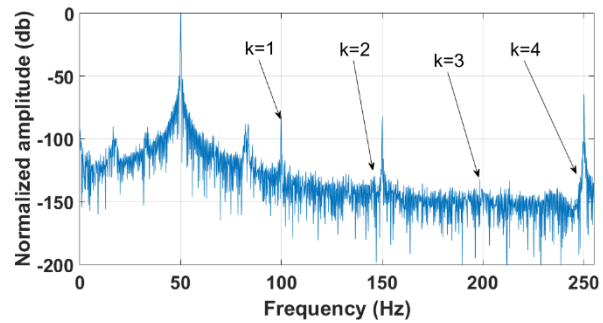
Fig. 9. Normalized spectrum of the IM's current for level-2 misalignment condition
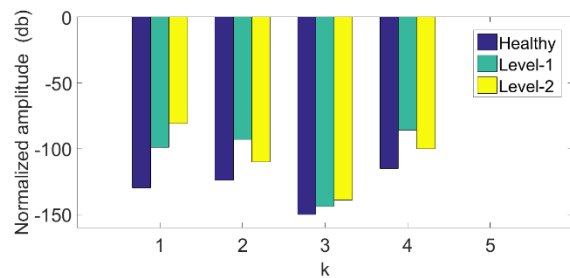
Fig. 10. Normalized amplitude of the harmonics of the IM's current in the healthy condition, and level-1 and level-2 misalignment

In Fig. 11 to Fig. 13, the current signal of the BLDC motor in the frequency domain is shown for healthy condition, and level-1 and level-2 misalignment. The results indicate that for fault conditions the amplitude of the characteristic frequencies was increased in comparison to the healthy condition. Among these harmonics, the first two harmonics reequip equated to $K = -1$ and $K = 1$ have more amplitude changes, with

amplitude of -55db and -47db for level-1, and amplitude of -53db and -46db for level-2. These harmonics have the highest amplitude among the fault frequencies and can easily be separated from healthy conditions. The amplitude of the harmonics (-4 to 4) in the healthy, level-1 fault and level-2 fault is specified in Fig. 14. A comparison of Figs 14 and 10 shows that the fault frequency characteristics around the main frequency are better separated from the healthy condition in the BLDC motor than in the IM.
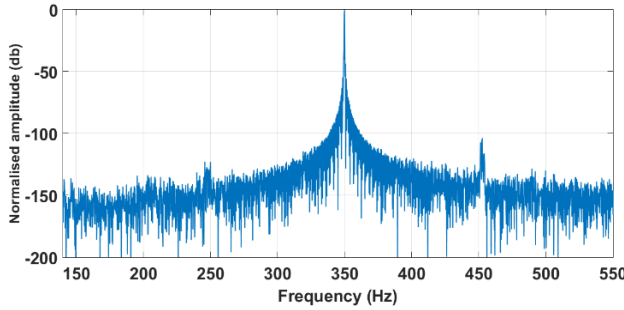
Fig. 11. Normalized spectrum of the BLDC current for the healthy condition
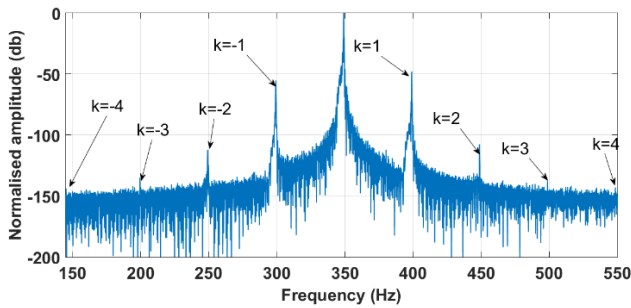
Fig.12. Normalized spectrum of the BLDC current for level-1 misalignment
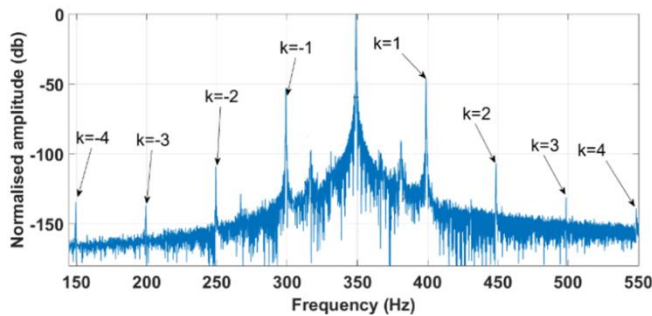
Fig. 13. Normalized spectrum of the BLDC current for level-2 misalignment
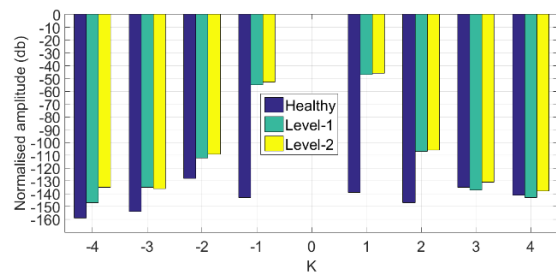
Fig. 14. Normalized amplitude of the harmonics of the BLDC motor's current in the healthy condition, and level-1 and level-2 misalignment

Therefore, it can be concluded that it is possible to detect the parallel misalignment between the driver machine and the load, using the FFT analysis of the BLDC motor's current.

B. Wavelet Packet Transform

For five stages in WPT, the current signal was divided into approximate and detailed signals using the Daubechies 8 mother wavelet. The frequency content of the current signal was split into 32 sub-bands in the fifth stage of the WPT. The frequency spectrum of each sub-band at step 5 is displayed in Table III.

TABLE III
The Frequency Ranges of Each Sub-Band for Step 5

sub-band	Frequency range (Hz)	sub-band	Frequency range (Hz)
$d_{5.0}(t)$	0-78	$d_{5.16}(t)$	1248-1326
$d_{5.1}(t)$	78-156	$d_{5.17}(t)$	1326-1404
$d_{5.2}(t)$	156-234	$d_{5.18}(t)$	1404-1482
$d_{5.3}(t)$	234-312	$d_{5.19}(t)$	1482-1560
$d_{5.4}(t)$	312-390	$d_{5.20}(t)$	1560-1638
$d_{5.5}(t)$	390-468	$d_{5.21}(t)$	1638-1716
$d_{5.6}(t)$	468-546	$d_{5.22}(t)$	1716-1794
$d_{5.7}(t)$	546-624	$d_{5.23}(t)$	1794-1872
$d_{5.8}(t)$	624-702	$d_{5.24}(t)$	1872-1950
$d_{5.9}(t)$	702-780	$d_{5.25}(t)$	1950-2028
$d_{5.10}(t)$	780-858	$d_{5.26}(t)$	2028-2106
$d_{5.11}(t)$	858-936	$d_{5.27}(t)$	2106-2184
$d_{5.12}(t)$	936-1014	$d_{5.28}(t)$	2184-2262
$d_{5.13}(t)$	1014-1092	$d_{5.29}(t)$	2262-2340
$d_{5.14}(t)$	1092-1170	$d_{5.30}(t)$	2340-2418
$d_{5.15}(t)$	1170-1248	$d_{5.31}(t)$	2418-2500

From the FFT analysis, it was found that the best characteristic frequency for the IM to detect the misalignment fault is 99.7 Hz. This frequency is in the sub-band $d_{5.1}(t)$. Fig.15 shows the time domain diagram of sub-band $d_{5.1}(t)$ for the IM current signal in healthy conditions and misaligned conditions.
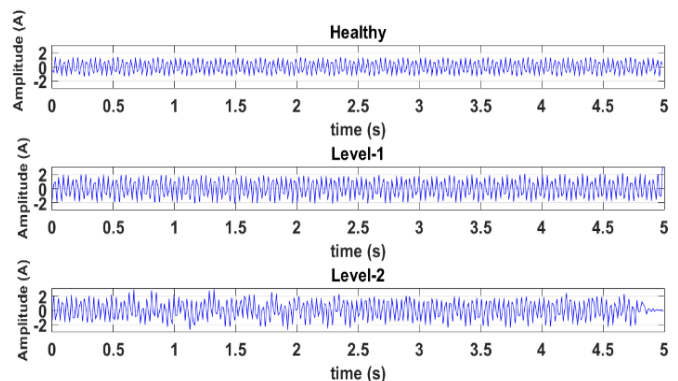
Fig. 15. Detail coefficient $d_{5.1}(t)$ for IM current in the healthy condition, and level-1 and level-2 fault conditions

Also, the frequencies 298.45Hz and 397.94Hz are the best characteristic frequencies to detect the misalignment fault through the current signal of the BLDC motor. These frequencies are in the sub-bands $d_{5.3}(t)$ and $d_{5.5}(t)$ of the WPT. Because both sub-bands provide similar results, only the sub-band $d_{5.3}(t)$ was used for the analysis. Fig. 16 shows the comparison between the BLDC current signals of the healthy condition, and level-1 and level-2 fault conditions for the sub-band $d_{5.3}(t)$.
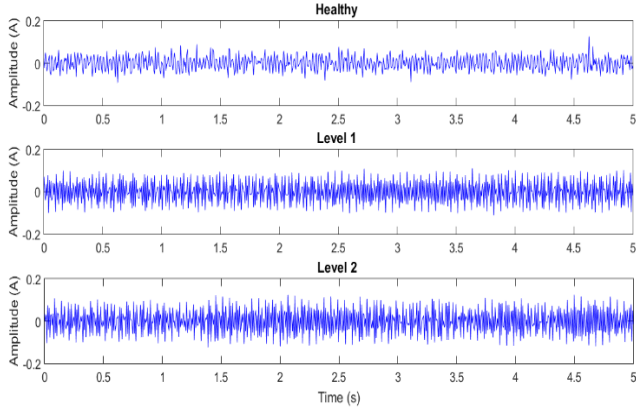
Fig. 16. Detail coefficient $d_{5.3}(t)$ for BLDC current in the healthy condition, and level-1 and level-2 fault conditions

Figs 15 and 16 demonstrate that the energy of the current signal increases by the misalignment fault. The increase in the energy of the signal lead to a diagnostic method based on sub-band energy. The sub-band signal energy and the normalized energy can be calculated as follows:

$$the \ E_{jn} = \sum_t (d_{j,n}(t))^2 \tag{7}$$

$$equal E_{jn,N} = \frac{E_{jn}}{E_{Ave}} \tag{8}$$

Here $d_{i,j}$ is the sub-band of the original signal, and E_{jn} is the energy of the sub-band. In addition, E_{Ave} is the average energy of the original signal in healthy conditions. Fig. 17 shows the normalized energy of sub-band $d_{5.1}(t)$ for IM's current signal. Also, Fig. 18 shows the normalized energy of sub-band $d_{5.3}(t)$ for the BLDC motor's current signal. From tig.17 and Fig.18, it is obvious that for both IM and BLDC motors the amount of normalized energy E_{sb_Norm} in fault condition is higher than the health conditions. Comparing Fig. 17 and Fig. 18 demonstrates that the energy of the current signal in IM increases with the increase of the load, while for the BLDC motor the energy of the current signal decreases with the increase of the load. The reason for this phenomenon is that with an increase in the load, the IM's current increases to produce more power. At the same time, the speed of the IM and the BLDC motor decreases. Therefore, because the BLDC motor acts as a generator its current decreases. As it is clear in Fig. 17 and Fig. 18, this method has well separated the misalignment fault from the healthy state.
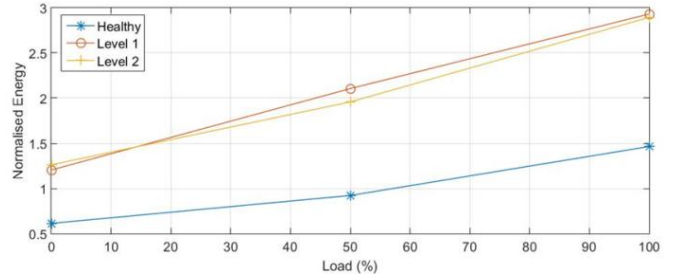
Fig. 17. Normalized energy $d_{5.1}(t)$ for IM current in the healthy, level-1 fault and level-2 fault conditions at different loads
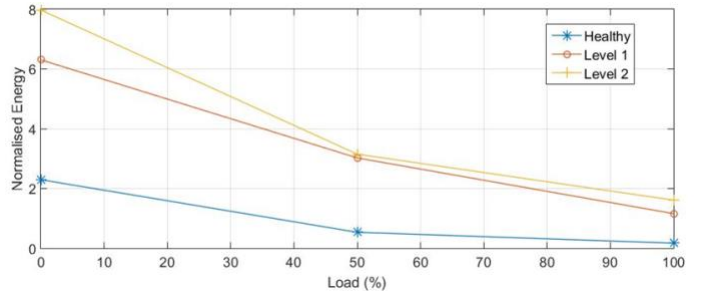
Fig. 18. Normalized energy $d_{5.3}(t)$ for BLDC current in the healthy, level-1 fault and level-2 fault conditions at different loads

V. CONCLUSION

These days, many factories and industries have rotating machinery that is constantly in use, and any one of these systems' failure can seriously harm the entire industry. As a result, it is essential to watch the condition of such systems. The MCSA technique is the most cost-effective way to monitor the condition of a rotating machine. However, due to the fact that multi-MW scale motors with a high current range require sensors with a higher resistance, which in turn raises the cost, this technique cannot be used for all rotating systems. Second, it is challenging to handle current signals because noise brought on by voltage fluctuations is present in the direct current drawn from the induction motor. Thirdly, there are rotating systems used in some industries that do not operate with electric current, and thereby it is not possible to use MCSA. In this study, a small BLDC motor was coupled to a rotating system and the current signal of the BLDC was measured. This signal was analyzed by two different methods including Fast Fourier Transform and wavelet packet transform. The results indicated that both methods are capable to distinguish the parallel misalignment between the driver and the load.

VI. REFERENCES

[1] Verma, A.K., Sarangi, S. and Kolekar, M.H., 2013. Misalignment fault detection in induction motor using rotor shaft vibration and stator current signature analysis. *International Journal of Mechatronics and Manufacturing Systems*, 6(5-6), pp.422-436.

[2] Bossio, J.M., Bossio, G.R. and De Angelo, C.H., 2009, November. Angular misalignment in induction motors with flexible coupling. In *2009 35th Annual Conference of IEEE Industrial Electronics* (pp. 1033-1038). IEEE.

[3] Gibbons, C.B., 1976. Coupling misalignment forces. In *Proceedings of the 5th Turbomachinery Symposium*. Texas A&M University. Gas Turbine Laboratories.

[4] Sinha, J.K., Lees, A.W. and Friswell, M.I., 2004. Estimating unbalance and misalignment of a flexible rotating machine from a single run-down. *Journal of Sound and Vibration*, 272(3-5), pp.967-989.

[5] Prabhu, B.S., 1997. An experimental investigation on the misalignment effects in journal bearings. *Tribology transactions*, *40*(2), pp.235-242.

[6] Bahaloo, H., Ebrahimi, A. and Samadi, M., 2009, January. Misalignment modeling in rotating systems. In *Turbo Expo: Power for Land, Sea, and Air* (Vol. 48876, pp. 973-979).

[7] Chacon, J.L.F., Andicoberry, E.A., Kappatos, V., Asfis, G., Gan, T.H. and Balachandran, W., 2014. Shaft angular misalignment detection using acoustic emission. *Applied acoustics*, *85*, pp.12-22.

[8] Caso, E., Fernandez-del-Rincon, A., Garcia, P., Iglesias, M. and Viadero, F., 2020. Monitoring of misalignment in low speed geared shafts with acoustic emission sensors. *Applied Acoustics*, *159*, p.107092.

[9] Chacon, J.L.F., Andicoberry, E.A., Kappatos, V., Asfis, G., Gan, T.H. and Balachandran, W., 2014. Shaft angular misalignment detection using acoustic emission. *Applied acoustics*, *85*, pp.12-22.

[10] Khan, M.A., Shahid, M.A., Ahmed, S.A., Khan, S.Z., Khan, K.A., Ali, S.A. and Tariq, M., 2019. Gear misalignment diagnosis using statistical features of vibration and airborne sound spectrums. *Measurement*, *145*, pp.419-435.

[11] Sarkar, S., Nandi, A., Neogy, S., Dutt, J.K. and Kundra, T.K., 2010. Finite element analysis of misaligned rotors on oil-film bearings. *Sadhana*, *35*(1), pp.45-61.

[12] Xu, M. and Marangoni, R.D., 1994. Vibration analysis of a motor-flexible coupling-rotor system subject to misalignment and unbalance, part I: theoretical model and analysis. *Journal of sound and vibration*, *176*(5), pp.663-679.

[13] Hili, M.A., Fakhfakh, T., Hammami, L. and Haddar, M., 2005. Shaft misalignment effect on bearings dynamical behavior. *The International Journal of Advanced Manufacturing Technology*, *26*(5-6), pp.615-622.

[14] Verucchi, C., Bossio, J., Bossio, G. and Acosta, G., 2016. Misalignment detection in induction motors with flexible coupling by means of estimated torque analysis and MCSA. *Mechanical Systems and Signal Processing*, *80*, pp.570-581.

[15] Chaudhury, S.B., Sengupta, M. and Mukherjee, K., 2013. Experimental study of induction motor misalignment and its online detection through data fusion. *IET Electric Power Applications*, *7*(1), pp.58-67.

[16] Vilchis-Rodriguez, D.S., Djurović, S. and Smith, A.C., 2013. Wound rotor induction generator bearing fault modelling and detection using stator current analysis. *IET Renewable Power Generation*, *7*(4), pp.330-340.

[17] Jung, J., Park, Y., Lee, S.B., Cho, C.H., Kim, K., Wiedenbrug, E.J. and Teska, M., 2017. Monitoring journal-bearing faults: making use of motor current signature analysis for induction motors. *IEEE Industry Applications Magazine*, *23*(4), pp.12-21.

[18] Kar, C. and Mohanty, A.R., 2008. Vibration and current transient monitoring for gearbox fault detection using multiresolution Fourier transform. *Journal of Sound and Vibration*, *311*(1-2), pp.109-132.

[19] Chen, X. and Feng, Z., 2019. Time-frequency space vector modulus analysis of motor current for planetary gearbox fault diagnosis under variable speed conditions. *Mechanical Systems and Signal Processing*, *121*, pp.636-654.

[20] Antonino-Daviu, J. and Popaleny, P., 2018, September. Detection of induction motor coupling unbalanced and misalignment via advanced transient current signature analysis. In *2018 XIII International Conference on Electrical Machines (ICEM)* (pp. 2359-2364). IEEE.

[21] Randall, R.B., 2011. Vibration-based condition monitoring: industrial, aerospace and automotive applications. John Wiley & Sons.

[22] Verma, A.K., Sarangi, S. and Kolekar, M.H., 2014. Experimental investigation of misalignment effects on rotor shaft vibration and on stator current signature. *Journal of Failure Analysis and Prevention*, *14*(2), pp.125-138.

[23] Rajagopalan, S., 2006. *Detection of Rotor and Load Faults in BLDC Motors Operating Under Stationary and Non-Stationary Conditions* (Doctoral dissertation, Georgia Institute of Technology).

[24] Arkan, M.Ü.S.L.Ü.M., Çaliş, H. and Tağluk, M.E., 2005. Bearing and misalignment fault detection in induction motors by using the space vector angular fluctuation signal. *Electrical Engineering*, *87*(4), pp.197-206.

[25] Zhou, R., Bao, W., Li, N., Huang, X. and Yu, D., 2010. Mechanical equipment fault diagnosis based on redundant second-generation wavelet packet transform. *Digital signal processing*, *20*(1), pp.276-288.

[26] Zarei, J. and Poshtan, J., 2007. Bearing fault detection using wavelet packet transform of induction motor stator current. *Tribology International*, *40*(5), pp.763-769.

[27] Ye, Z., Wu, B. and Sadeghian, A., 2003. Current signature analysis of induction motor mechanical faults by wavelet packet decomposition. *IEEE transactions on industrial electronics*, *50*(6), pp.1217-1228.

[28] Jiang, H., Li, C. and Li, H., 2013. An improved EEMD with multiwavelet packet for rotating machinery multi-fault diagnosis. *Mechanical Systems and Signal Processing*, *36*(2), pp.225-239.

[29] Yan, R., Gao, R.X. and Chen, X., 2014. Wavelets for fault diagnosis of rotary machines: A review with applications. *Signal processing*, *96*, pp.1-15.